Accepted Article

Original Article

Pannexin-1 and P2X7-receptor are required for apoptotic osteocytes in fatigued bone to trigger RANKL production in neighboring bystander osteocytes†

Wing Yee Cheung[1], J. Christopher Fritton[2], StacyAnn Morgan[1], Zeynep Seref-Ferlengez[1], Jelena Basta-Pljakic[1], Mia M. Thi[3,4], Sylvia O. Suadicani[3], David C. Spray[3], Robert J. Majeska[1], and Mitchell B Schaffler[1,+]

[1] Department of Biomedical Engineering, City College of New York

[2] Department of Orthopaedic Surgery, New Jersey Medical School, Rutgers University

[3,4]Departments of Orthopaedic Surgery, Urology, and Neuroscience, Albert Einstein College of Medicine and Montefiore Medical Center

[+]Correspondence:
Mitchell B Schaffler, PhD
Department of Biomedical Engineering
The City College of New York
160 Convent Avenue
New York, NY 10031
212-650-5070
mschaffler@ccny.cuny.edu

†This article has been accepted for publication and undergone full peer review but has not been through the copyediting, typesetting, pagination and proofreading process, which may lead to differences between this version and the Version of Record. Please cite this article as doi: [10.1002/jbmr.2740]

Initial Date Submitted July 21, 2015; Date Revision Submitted November 5, 2015; Date Final Disposition Set November 8, 2015

Journal of Bone and Mineral Research
This article is protected by copyright. All rights reserved
DOI 10.1002/jbmr.2740

This article is protected by copyright. All rights reserved

Accepted Article

Abstract:

Osteocyte apoptosis is required to induce intracortical bone remodeling following microdamage in animal models, but how apoptotic osteocytes signal neighboring "bystander" cells to initiate the remodeling process is unknown. Apoptosis has been shown to open pannexin-1 (Panx1) channels to release ATP as a "find-me" signal for phagocytic cells. To address whether apoptotic osteocytes use this signaling mechanism, we adapted the rat ulnar fatigue-loading model to reproducibly introduce microdamage into mouse cortical bone and measured subsequent changes in osteocyte apoptosis, RANKL expression and osteoclastic bone resorption in wild type (WT, C57Bl/6) mice and in mice genetically deficient in Panx1 (Panx1KO). Mouse ulnar-loading produced linear microcracks comparable in number and location to the rat model. WT mice showed increased osteocyte apoptosis and RANKL expression at microdamage sites at 3 days after loading, and increased intracortical remodeling and endocortical tunneling at day 14. With fatigue, Panx1KO mice exhibited levels of microdamage and osteocyte apoptosis identical to WT mice. However, they did not upregulate RANKL in bystander osteocytes or initiate resorption. Panx1 interacts with $P2X_7R$ in ATP release; thus we examined $P2X_7R$-deficient mice and WT mice treated with $P2X_7R$ antagonist Brilliant Blue G (BBG) to test the possible role of ATP as a find-me signal. $P2X_7RKO$ mice failed to upregulate RANKL in osteocytes or induce resorption despite normally elevated osteocyte apoptosis after fatigue loading. Similarly, treatment of fatigued C57Bl/6 mice with BBG mimicked behavior of both Panx1KO and $P2X_7RKO$ mice; BBG had no effect on osteocyte apoptosis in fatigued bone, but completely prevented increases in bystander osteocyte RANKL expression and attenuated activation of resorption by more than 50 percent. These results indicate that activation of Panx1 and $P2X_7R$ are required for apoptotic osteocytes in fatigued bone to trigger RANKL production in neighboring bystander osteocytes and implicate ATP as an essential signal mediating this process. This article is protected by copyright. All rights reserved

Accepted Article

Introduction

It is well established that osteocyte apoptosis – whether due to fatigue microdamage, estrogen loss or disuse – triggers bone remodeling [1-4]. In each of these instances, the initiation of bone remodeling was preceded by osteocyte apoptosis in the region of bone that is subsequently remodeled [1-4]. Moreover, this osteocyte apoptosis is essential for remodeling to occur; preventing apoptotic cell death by use of a pan-caspase inhibitor completely blocked the initiation of bone resorption [2,3,5]. In the bone immediately surrounding microdamage sites, where osteocyte apoptosis has been studied extensively, some 50 percent of osteocytes die [2,5,6]. However, Kennedy et al. recently discovered that the viable osteocytes near to the dying ones produce the essential osteoclastogenic signal receptor activator of nuclear factor-kappaB ligand (RANKL) [1]. Moreover, they found that osteocyte apoptosis at these sites, not the microdamage itself, triggers the neighboring viable osteocytes to produce RANKL [2]. This overall scenario resembles "bystander" cell signaling [7] wherein cells undergoing a "purposeful" (apoptotic) death trigger their surviving neighbors to recruit the specialized phagocytic cells needed to remove damaged cells/tissue and to initiate repair. Bystander signaling driven by apoptosis is commonly observed in healing of nonskeletal focal injuries. For example, in focal brain and heart ischemia, retinal, corneal and skin injury healing, most cells in the core of the lesions die by apoptosis regardless of the initial cause of injury [8-11].

The signals that emanate from dying osteocytes and stimulate osteoclastogenic cytokine expression in bystander osteocytes are not known. Speculations in the literature have revolved around signals (e.g., apoptotic debris, high mobility group box 1 protein (HMGB1) release) that arise from events occurring late in the cell death process [12-14], but *in vivo* data supporting these speculations are lacking. Moreover, the apoptotic osteocyte-induced RANKL upregulation in viable neighboring osteocytes begins early in the apoptosis process, which suggests that signals released acutely from dying osteocytes play a dominant role in inducing nearby osteocytes to produce osteoclastogenic cytokines.

This article is protected by copyright. All rights reserved

Accepted Article

Over the last decade, a number of seminal studies established that cells in the early stage of apoptosis, before overt signs of cell degradation are seen, release a number of 'find-me" signals that stimulate activation and migration of professional phagocytes which remove dying cells [15-19]. These are released early in the apoptotic process - well before cellular membrane integrity is compromised. The major soluble chemoattractant find-me signals released during the early phase of apoptosis that have been well defined in recent studies are nucleoside triphosphates (ATP and UTP), lysophosphatidylchloline (lysoPC) and the chemokine CX3CL1 [20-22]. These small molecules diffuse readily through the local tissue to bind to appropriate receptors on the responding cells. Among these major acute signals from apoptotic cells, ATP has high potential relevance to the activation of resorption, as it has been shown to upregulate RANKL in osteoblast-lineage cells [23,24]. In contrast, UTP regulates osteoclast survival, but not recruitment or differentiation [25]. CX3CL1 is involved with osteoclast differentiation (pre-osteoclasts express its receptor) but does not alter RANKL expression [26-28] and LysoPC inhibits osteoclast differentiation [29].

Recent studies demonstrated that release of an acute bolus of purinergic signaling molecules from apoptotic cells depends upon the same critical caspases that drive intracellular degradation. Specifically, during apoptosis there is an activated caspase 3-dependent opening of cell surface pannexin 1 (Panx1) channels, which are known to provide a conduit for controlled cellular ATP release in various cell types, including bone cells. Panx1 is a member of the pannexin family of transmembrane channel-forming proteins that are homologous to invertebrate gap junction proteins, the innexins [30]. However, Panx1 forms only non-junctional channels (i.e., "hemichannels") that allow exchange of small molecules between the cytoplasm and the extracellular space [31-35]. Panx1 channels are unique in that they are not only voltage sensitive, but also open in response to mechanical stimulation, elevation in extracellular K^+ and activation of cell surface receptors, in particular the ionotropic $P2X_7$ receptor ($P2X_7R$).

These findings and the fact that osteocytes co-express Panx1 and $P2X_7R$ [36,37] coupled with the evidence of caspase-dependent Panx1 channel opening during apoptosis [38], led us to ask whether apoptotic osteocytes may communicate with bystander osteocytes via bolus ATP released through

This article is protected by copyright. All rights reserved

Panx1 channels, and if this ATP release plays a significant role in activation of osteocyte RANKL expression in bystander osteocytes. To test this hypothesis we adapted our rat ulnar end-loading fatigue model [39] to induce bone microdamage in mouse ulnae. Given the demonstrated functional interplay of Panx1 with $P2X_7R$ in mechanisms of cellular ATP release [40-43], the possible role of ATP as a find-me signal from activation of the $P2X_7R$-Panx1 functional complex in bone was also tested by inducing fatigue microdamage in $P2X_7R$-deficient mice and pharmacologically in fatigue loaded WT mice treated with the $P2X_7R$ antagonist Brilliant Blue G.

MATERIALS AND METHODS

1. Development of the Mouse Ulnar Fatigue Model

1.a.: Model development: The rat ulnar fatigue model originally developed in our laboratory [39] was modified for use with mice. Importantly, strain-controlled loading, rather than force-controlled loading, was used to determine precisely when the test should be stopped before microcracks propagated and merged to create an overt fracture. Strain- or displacement-controlled fatigue loading slows accumulation of microdamage compared to force-controlled loading, as the loading force applied under strain control decreases as matrix damage occurs; this slows cracking [44,45]. Since bone microcracks (μcracks) are typically 30-100 μm long [39,46] and the mouse diaphyseal cortex is about 200 μm wide, there is little margin for error during loading. Using this strain controlled approach, where load and energy decrease, we were able to reliably stop fatigue loading without breaking the ulnae, and thereby introduce small numbers of μcracks into diaphyseal cortex (comparable to our studies in rat ulnae).

Model development studies were performed in 4-5 month old, female C57Bl/6 (B6) mice (Jackson Labs, Bar Harbor ME). Calibration studies were performed to determine the load-strain-displacement characteristics of B6 mouse ulnae, following the procedures detailed elsewhere [39]. Once completed for B6 ulnae, similar calibration studies were performed for ulnae of the knockout strains used in the second part of these studies (see below).

This article is protected by copyright. All rights reserved

Accepted Article

1.b: Fatigue studies Mice were anesthetized with isoflurane (0.5-2%), forelimbs were positioned into the load path in an electromagnetic axial loading system (Electroforce 3200, Bose Corp, MN, USA) with the elbow and volar flexed carpus placed into brass cups of the loading system. Limbs were pre-loaded at 2 Hz for 50 cycles at 0.5 N (~250 μstrain) to allow the bone to settle into position. Forelimbs were then cyclically loaded under displacement control at levels that we had determined in our calibration studies to cause strains of ~3000 ± 500 μstrain at the mid-diaphysis. Loading was continued at 2 Hz until the bone lost 15% of its original stiffness, as measured from the decrease in loading force. This single damage endpoint was determined in preliminary studies to produce microdamage levels comparable to that seen in the rat ulnar fatigue model, and to activate cortical bone resorption. After loading, mice were either given buprenorphine analgesia and returned to their cages for Survival studies or sacrificed immediately to assess Acute microdamage. For Survival studies, mice ambulated normally and were allowed ad libitum access to food and water for the duration of the study. For these initial studies to define the mouse ulnar fatigue model, ulnae in 4-5 month old B6 female mice (n=6 per group) were subjected to fatigue loading as described above. Ulnae were examined immediately after loading and at 3 and 14 days after loading to assess osteocyte signaling and osteoclastic resorption events, respectively. All procedures were performed under IACUC approvals from the City College of New York and the Albert Einstein College of Medicine.

Microdamage and Resorption resulting from this fatigue loading was assessed as in our previous studies [39]. Ulnae and radii were dissected together and fixed in 10% neutral buffered formalin. Forelimbs were stained en bloc with basic fuchsin and embedded in PMMA. Cross sections were cut with a diamond saw polished to 80 μm and examined light microscopy to measure microcrack numbers (Cr.N, #/mm^2); measurements were restricted to typical linear microcracks with sharp, well defined edges. Toluidine blue stained sections were used to assess intracortical resorption activity, measured as resorption space number (Rs.N, #/mm^2). In addition, we found that new remodeling units tunnel into the mouse ulnar cortex from the endocortical surface; thus the number of discrete new tunneling foci emanating from the endocortical surface (En.Tun.N, #/mm) was measured as well.

This article is protected by copyright. All rights reserved

Accepted Article

Accepted Article

Osteocyte Apoptosis and RANKL Expression were examined in ulnar cross-sections using immunohistochemistry (IHC). Ulnae were decalcified with formic acid, dehydrated in ethylene glycol monoethyl ether and embedded in paraffin. Cross-sections (5 μm) from the damage region of the mid-diaphysis were deparaffinized, rehydrated, and endogenous tissue peroxidases quenched using 3% hydrogen peroxide. IHC studies were performed using procedures detailed elsewhere [1,2,5]. Briefly, sections were then treated with a methanol-NaOH based antigen retrieval solution (DeCal Antigen Retrieval, BioGenex, California), blocked with 2.5% Horse Serum (ImmPress Reagent Kit, MP-7405, Vector Laboratories, Burlingame, CA) prior to overnight incubation at 4°C with primary antibodies against cleaved caspase-3 to detect apoptotic osteocyte (1:200, Cell Signaling Technologies, 9661) or RANKL (1:200, Santa-Cruz Biotechnologies, SC-7628). Detection was performed using anti-rabbit secondary antibody (MP-4701 for cleaved caspase-3), or anti-goat secondary antibody (MP-7405 for RANKL) for 30 minutes, followed by a DAB-horseradish peroxidase substrate detection system (ImmPact DAB, SK-4105). Chondrocytes within the femoral growth plates of WT mice were used as positive controls to detect expression of cleaved caspase 3 and RANKL.

Histomorphometry: Numerous studies have established that osteocyte apoptosis at microdamage sites is highly localized to within about 150 microns of the damage site; osteocyte apoptosis levels outside the damage areas are the same as in non-loaded control bones [1,2,5,6,47]. Accordingly, numbers of apoptotic and RANKL-expressing osteocytes were measured in damage-containing (MDX) and in the non-damaged (NON-MDX) of the ulnar cortex (Fig 1); data for both damage locations within a bone were averaged together. Caspase-3 and RANKL positive osteocytes were counted and expressed as a percentage of total number of osteocytes in each region (%Casp3+ Ot, %RANKL+ Ot). Measurements were made by a single observer (WYC), who was blinded to specimen identity. Random sections were also counted by a second observer (MBS) to assure consistency. All osteocyte measurements were made in 3-day post-fatigue ulnae. Data were quantified using Image J (NIH).

This article is protected by copyright. All rights reserved

2. Involvement of Panx1 and P2X$_7$R on osteocyte apoptosis, osteocyte RANKL expression and bone remodeling after fatigue. 2.a.: Knockout mouse studies: We used Panx1 deficient mice (Panx1$^{tm1a(KOMP)Wtsi}$), generated by the Knockout Mouse Project (KOMP, www.KOMP.org) in C57Bl/6 mice to test the hypothesis that Panx1 is required for apoptosis induced expression of osteocyte RANKL. This is a global knockout of the ubiquitously expressed pannexin Panx1[48]. The Panx1 knockout mouse (Panx1KO) was constructed by using the knockout-first strategy described by Testa et al [49]. Panx1KO mice exhibit approximately 70% reduction in Panx1 mRNA expression in tissues, but behave as a functional Panx1 knockout as the channel protein expression is reduced even more severely [48]. In contrast to standard KO designs using targeted deletions, the KO-first approach used in these mice leaves the *Panx1* gene intact and rather truncates the *Panx1* mRNA, and thus these mice actually represent a hypomorph but are typically referred to in the literature as KO [48]. The Panx1KO mice (Jackson Laboratories, C57/Bl6 background) grow normally and thrive well. Interestingly, Panx1KO mice have a macrophage recruitment defect that is evident with challenge [50,51]. Pannexin-1 is a major ATP release channel, is expressed in all cells [52] and is associated with the purinergic receptor P2X$_7$R. Accordingly, we examined P2X$_7$RKO mice to assess how this receptor might mediate effects of ATP released via Panx1 channels. P2X$_7$RKO mice (B6.129P2-*P2rx7*^{tm1Gab}/J back-crossed onto C57Bl/6 background) and wild type (WT) B6 mice were obtained from Jackson Laboratories. The skeletal biology of this P2X$_7$RKO strain was previously described in detail by Li et al [53]. Osteocyte expression of the P2X$_7$R has been previously reported [53-55]. Both Panx1KO and P2X$_7$RKO mice were maintained at Albert College of Medicine until they reached skeletal maturity. All mice were fed with normal chow, housed 2-5 to a cage, maintained at a 12/12 hour light-dark cycle, and allowed to roam freely in cages before and after fatigue loading. Studies used 4-6 mice per group at each time point (Acute and Survival: 3 and 14 days).

2.b.: *MicroCT studies* were performed to assess the baseline bone architecture in Panx1- and P2X$_7$R-deficient mice. Femora of 4-5 month old female WT and KO mice (same mice used in loading studies) were scanned at 6.7μm resolution with a SkyScan 1172 microCT system (SKY SCAN, Kontich, Belgium). Images were acquired using a 10-MP digital detector, at 100 KV and 100 mA and using a

This article is protected by copyright. All rights reserved

0.5-mm aluminum filter. Flat field calibration was performed prior to each scanning session. X-ray projections were generated from each sample at 0.3 degrees; five exposures per projection were taken (1767-ms exposure time). A global threshold was applied to images using gray scale values of 85 and 70 for cortical and trabecular bone, respectively. Images were reconstructed to generate cross section images from X-ray projections (NRecon, V1.6.6.0). Reconstruction procedures implemented a standard post-alignment compensation algorithm to eliminate misalignment artifacts, and all reconstruction parameters (kernel size 1 for asymmetrical boxcar window, ring artifact 10, beam hardening 40%) were kept constant throughout each scan reconstruction. Measurements were performed at the mid-diaphysis.

2.c.: Osteocyte marker gene expression: Gene expression was assessed in contralateral femora from those used for histology. Femora were thoroughly cleaned of muscle and periosteal tissue, the bone marrow was flushed out from a 5 mm long mid-diaphyseal segment and the resulting cortical bone samples were immediately flash-frozen in liquid nitrogen The cortical bone samples produced in this manner are highly enriched in osteocytes. Bones were homogenized (Mikro-Dismembranator, Sartorius, Germany) and RNA was purified with QiaShredder and RNEasy mini-kits with DNAase, according to the manufacturer's protocol (Qiagen, Valencia, CA). Quantity and quality of RNA were determined by absorbance (Biotek, Winooski, VT and cDNA was synthesized from mixed primers (Quantitect Reverse Transcription Kit, Qiagen). cDNA's (12.5 ng each) were analyzed by real-time PCR using a SYBR green detection system to determine relative expressions of dentin matrix protein-1 (*DMP1*), sclerostin (*SOST*), *RANKL* and *OPG* in knockout and wild type mouse cortical bone; 18s RNA was used a housekeeping gene. Forward and reverse primer sequences were:

DMP1 – ACGACAGTGAGGATGAGGCA / ATCGCTCCTGGTACTCTCGG;
SOST – CTTCAGGAATGATGCCACAGAGGT / ATCTTTGGCGTCATAGGGATGGTG;
RANKL – ACGCAGATTTGCAGGACTCG / GGGCCACATCCAACCATGAG;
OPG – TGGACCAAAGTGAATGCCG / GGGCCACATCCAACCATGAG;
18S – CACGGCCGGTACAGTGAAAC / AGAGGAGCGAGCGACCAAA.

This article is protected by copyright. All rights reserved

3. Remodeling and osteocyte reactions in response to fatigue in Panx1KO and P2X$_7$RKO mice Ulnae in Panx1KO, P2X$_7$RKO and WT mice were subjected to fatigue loading as described above and examined at 3 and 14 days after loading to assess osteocyte signaling and osteoclastic resorption events, respectively. Displacements/loads required were ~10% lower in P2X$_7$RKO than in the WT or Panx1KO mice, consistent with their smaller cross-sectional dimensions as reported by Li et al., and also observed in our studies [53]. In an additional confirmatory experiment, fatigued and non-loaded B6 (wild-type) mice (4-5 m.o, female, n= 6/group) were injected with the P2X$_7$R antagonist Brilliant Blue G (BBG: 50 mg/kg, IP, Sigma, St Louis, MO, [56-58] or PBS vehicle once daily for 3 days or 14 days starting at the time of fatigue to pharmacologically test the relevance of the ATP signaling axis in apoptotic osteocyte triggering of RANKL expression in their viable neighbors and the effect on cortical bone resorption, respectively. Osteocyte apoptosis, osteocyte RANKL expression and cortical bone resorption were examined as described above

4. Statistical analysis: Data are reported as mean ± standard deviation. GraphPad Statistical software was used to perform statistical tests. The Kruskal-Wallis ANOVA was used to test for differences among groups for numbers of caspase-3 or RANKL positive osteocytes in MDX or NON-MDX areas of WT vs Panx1 KO mice; WT vs P2X$_7$RKO mice or BBG-treated mice vs vehicle-treated mice. Dunn's test was used for post-hoc comparison. The Mann-Whitney U test was used to test differences in bone phenotype, resorption numbers and endocortical tunneling foci in comparisons between WT vs Panx1KO and WT vs P2X$_7$RKO mice.

RESULTS

1. Bone remodeling, osteocyte apoptosis and RANKL expression in the mouse ulnar cortex in response to fatigue loading In vivo fatigue loading of ulnae in B6 mice to the single damage endpoint used in these studies produced typical linear microdamage, within highly reproducible regions of the ulnar cortex and did not cause overt fracture (Fig 1A). This damage was localized to the regions approximately 1 mm distal to the mid-diaphysis, which is the region with the smallest diameter in the

This article is protected by copyright. All rights reserved

Accepted Article

mouse ulna. Within the ulnar cross-sections, microdamage occurred only in medial cortex regions (MDX regions, Fig 1A) and no microdamage was found in the lateral cortex (NON-MDX regions, Fig 1A), which is consistent with the localization of bone microdamage observed in the rat ulnar fatigue model [39]. Microcrack content in fatigued B6 ulnae was 3.1 ± 1.0/mm^2; no microcracks were present in the non-fatigued ulnae (Fig 1B; $p<0.0001$). Resorption was activated in fatigue loaded ulnae by 14 days after loading (Rs.N in fatigued ulnae = 2.5 ± 0.2/mm^2 vs 0 in nonloaded; Fig 1C); intracortical resorption spaces occurred only in the MDX regions and were not observed in the NON-MDX regions of loaded bone. In addition, discrete tunneling resorption foci were observed at endocortical surfaces at 14 days after fatigue loading (3.9 ± 1.9 /marrow cavity); these tunnels were absent from non-loaded ulnae (Fig 1D). Osteocyte apoptosis was dramatically elevated, approximately 5-fold over baseline levels in the microdamaged areas of the fatigued ulnar cortex (Fig 1E). Osteocyte apoptosis was unchanged from baseline in the non-damaged areas of cortex. Increased numbers of RANKL-expressing osteocytes were also seen only in the microdamaged areas of the cortex (Fig 1F).

2. Skeletal phenotype of Panx1KO and P2X$_7$RKO mice: MicroCT-studies bone revealed no differences in diaphyseal structure between Panx1KO and WT femora (Fig 2, indicating that under basal conditions the absence of Panx1 does not demonstrably alter skeletal properties). P2X$_7$RKO diaphyses were approximately 10% smaller in diameter and total cross-sectional area than WT bone (Fig 2). Knockout and WT mice showed similar gene expression levels of DMP1, SOST, RANKL and OPG in osteocyte enriched diaphyseal samples (data not shown).

3. *Bone remodeling, osteocyte apoptosis and RANKL expression in response to fatigue-loading in Panx1KO and P2X$_7$RKO mice* Microcrack content resulting from experimental fatigue loading was similar in all ulnae regardless of genotype (Cr.N: WT vs. Panx1KO: 3.1 ± 1.0/mm^2 vs. 3.8 ± 0.9/mm^2; WT vs, P2X$_7$RKO: 3.1 ± 1.0/mm^2 vs. 3.5 ± 0.9/mm^2). In contrast to WT mice, fatigued Panx1KO ulnae showed no activation of either intracortical resorption or endocortical tunneling resorption (Fig 3A,B). Osteocytes in microdamaged regions of Panx1KO mice ulnae underwent similar levels of apoptosis to WT mice (Fig 3C). In contrast, there was no increase of osteocyte RANKL expression in

This article is protected by copyright. All rights reserved

Accepted Article

fatigued bone in the absence of Panx1 (Fig 3C). The results were similar for deletion of $P2X_7R$. Levels of osteocyte apoptosis in fatigued bones were equivalent to those in fatigued WT ulnae, but no increases were seen in osteocyte RANKL expression (Fig 3C). Finally, we found that pharmacological blockade of the $P2X_7R$ in wild type B6 mice with BBG mimicked the behavior of both Panx1KO and $P2X_7RKO$ mice (Fig 4); BBG had no effect on osteocyte apoptosis in fatigued bone, but completely prevented the increases in osteocyte RANKL expression, and attenuated activation of endocortical and intracortical resorption by more than 50% ($p<0.05$ and $p<0.06$ respectively).

Discussion:

In this study, we showed using *in vivo* genetic approaches that Pannexin-1 channels do not influence osteocyte apoptosis in response to bone fatigue and microdamage, but these channels are required for the apoptotic osteocytes to trigger RANKL expression in neighboring bystander osteocytes and the initiation of osteoclastic bone remodeling. Bystander osteocytes in Panx1-deficient mice do not turn on RANKL expression with bone microdamage and osteocyte apoptosis *in vivo*. Furthermore, absence of Panx1 channels completely prevented normal activation of cortical bone remodeling in response to fatigue.

In the bone immediately surrounding microdamage sites, where osteocyte apoptosis has been studied extensively, some 50 percent of osteocytes die [1,2,5,6,47]. However, Verborgt et al. revealed that there are multiple osteocyte responses around microdamage sites [47]. They found that those osteocytes surrounding microdamage that do not undergo apoptosis actively respond by protecting themselves through increased production of anti-apoptotic and autophagy protein Bcl-2 [47]. Kennedy et al. in our laboratory recently discovered that the viable osteocytes nearby the dying ones produce the essential osteoclastogenic signal RANKL [1]. Moreover, in a subsequent report, Kennedy et al. found that it is the apoptotic osteocytes at these sites, not the microdamage, that trigger the neighboring viable osteocytes to produce RANKL [2]. If osteocyte apoptosis was pharmacologically blocked with a pan-caspase inhibitor, increases in RANKL expression in the bystander osteocytes is prevented – despite the presence of microdamage in the bone.

This article is protected by copyright. All rights reserved

Accepted Article

Speculations about potential signals from apoptotic osteocytes that can trigger and target osteoclast activation and recruitment have focused on events that occur and molecules that are released late in the cell death process (i.e. after membrane breakdown). Kogiannis [13] and Jilka [59] suggested that apoptotic bodies could be a potential signal from dying to neighboring osteocytes, as these particles stimulate existing osteoclasts on calvarial surfaces. However, our studies and others show that apoptotic bodies cannot serve as significant signal among osteocytes *in situ*, due to physical limitations. Apoptotic bodies are ~20-1000 nm in diameter while the molecular spacing in pericellular proteoglycan matrix surrounding osteocyte processes permits movement of solutes of 70,000 (≈ 6 nm diameter) [60]. A number of *in vitro* studies have shown that necrotic and apoptotic cells release several large intracellular proteins like HMGB1 [14,61]. Bidwell et al. showed that apoptotic MLO-Y4 cells release HMGB1, which stimulated TNFα and RANKL synthesis in bone marrow stromal cells [12,14,62]. *In vivo* confirmation of this mechanism is lacking. Moreover, recent data show that HMGB1 is released late in the apoptosis process, after cell membrane integrity is lost. [61,63] In contrast, we found that the onset of RANKL expression in bystander osteocytes occurs quickly (<24 hours) after bone fatigue, when early osteocyte apoptosis has started (i.e. caspases activated) but cell degradation is not yet present [1,2]. Thus, signals that are produced acutely by dying osteocytes play a dominant role in triggering RANKL expression in bystander osteocytes.

Over the last several years, a number of key studies established that cells in the early stages of apoptosis release a "find-me" chemoattractant signals that stimulate activation and migration of professional phagocytes which then remove dying cells [16,20-22,64,65]. These find-me signals are released early in the apoptotic process - well before cellular membrane integrity is compromised. Unlike the contact-based "eat-me" signals on cell membrane surfaces that allow phagocytic cells to identify early apoptotic cells (e.g. phosphatidylserine), these small find-me molecules diffuse readily through the local tissue to bind to appropriate receptors on the responding phagocytic lineage cells [16,20-22,64,65] . Among principal soluble chemoattractant find-me signals released during the early phase of apoptosis (ATP and UTP, lysoPC, CX3CL1), ATP has high potential relevance for resorption activation. ATP has been shown to upregulate RANKL in osteoblast-lineage cells [23,24]. In contrast, UTP influences

This article is protected by copyright. All rights reserved

Accepted Article

osteoclast survival, but not recruitment or differentiation (17). Hoshino et al (54) and Koizumi at al (72) have shown that CX3CL1 is involved with osteoclast differentiation (pre-osteoclasts express its receptor) but it does not alter RANKL expression. Kwak et al. demonstrated that LysoPC inhibits osteoclast differentiation [66].

In several elegant recent studies, Elliott et al. [20], Chekeni et al. [64] and Sandilos et al. [38] demonstrated that there is an acute bolus release of nucleotide "find-me" signaling molecules (ATP and UTP) from apoptotic cells. This release occurs through opening of Panx1 channels under the control of caspase-3 and -7 during apoptosis. Furthermore, they found that pharmacological blocking of Panx1 channels inhibits ATP and UTP release from apoptotic cells *and* decreases monocyte recruitment. Based on these observations, we tested whether Panx1 could similarly serve as a mediator of apoptotic osteocyte "find-me" signal release in bone as it does in other cell types. Furthermore, given that recruitment of osteoclasts, the professional phagocytic cells that remove apoptotic osteocytes, requires RANKL expression by bystander osteocytes, we asked whether apoptosis-dependent signal release from Panx1 channels might be a critical trigger for this localized upregulation of osteocyte RANKL production. We found that when microdamage was introduced into ulnae of Panx1-deficient mice, osteocyte apoptosis occurred at damage sites exactly as it does in WT bone. However, unlike in WT bone, this osteocyte apoptosis did not trigger RANKL production in the non-apoptotic bystander osteocytes in Panx1KO ulnae. Consequently, there was no activation of new resorption sites, confirming that Panx1 is required for apoptosis induced expression of osteocyte RANKL. These results further point to ATP as the essential signal that triggers surviving bystander osteocytes at microdamage sites to turn on RANKL. As discussed above, the apoptosis-driven opening of Panx1 channels releases high levels of ATP locally, and this ATP can serve as a potent activator and chemoattractant for macrophages.

We found that when the same fatigue challenge was applied to mice lacking the $P2X_7$ receptor, the results were identical to those for Panx1 deficiency, i.e. typical osteocyte apoptosis but no RANKL signaling by bystander osteocytes and no activation of cortical bone resorption. Pharmacological use of the $P2X_7R$ antagonist BBG produced the same osteocyte response. Further, BBG treatment resulted

This article is protected by copyright. All rights reserved

Accepted Article

in a marked reduction in the activation of new resorption sites at 14 days after fatigue. BBG suppression of resorption was not as complete as in the knockout mice. Indeed similarly attenuated results have reported for BBG treatment with neuronal injury *in vivo*. [57,58] Together these data point to the participation of both $P2X_7R$ and Panx1 in this bystander signaling and to ATP as the essential signal released from dying osteocytes that triggers surviving bystander osteocytes to turn on RANKL production in association with fatigue and microdamage.

How Panx1 and $P2X_7R$ may interact in apoptosis-dependent ATP signaling between dying and locally surviving osteocytes is not yet clear. Since osteocytes express both Panx1 and $P2X_7R$, the most straightforward scenario would be a paracrine mechanism wherein ATP released via Casp3-mediated opening of Panx1 channels in apoptotic osteocytes activates $P2X_7Rs$ on bystander osteocytes. This would not only trigger production of RANKL and other pro-osteoclastogenic signals but also amplify the apoptosis–initiated ATP signaling via $P2X_7R$-mediated activation of Panx1 channels in bystander osteocytes. ATP was previously shown to stimulate RANKL expression in osteoblast-lineage cells [23,24]. However, we cannot exclude additional mechanisms, e.g. involving same-cell (autocrine) ATP signaling or signaling via other receptors such as P2Y, which are expressed on osteoblasts [67] and were reported to mediate upregulation of RANKL [68].

Given the clear failure of Panx1KO mice to upregulate RANKL and initiate resorption in response to skeletal microdamage, the absence of a demonstrable skeletal phenotype without a remodeling stimulus was notable. Based on microCT examination (including trabecular bone, data not shown) and histological patterns, it was clear that Panx1KO osteoclasts carried out normal bone modeling and remodeling processes during development. This normal "baseline" skeletal phenotype of Panx1-deficient mice may result in part because the mice are hypomorphic Panx1 expressors rather than complete knockouts [48]. This may also contribute to their ability to grow normally despite neurological differences from wild type, i.e. diminished seizure threshold [69] and diminished pain sensitivity [70]. Interestingly, Panx1-deficient mice also exhibit a defect in macrophage recruitment that is evident following strong inflammatory challenge; this deficiency, however, is not seen in the normal day-to-day immune functions of these mice [51]. Unlike Panx1KO mice, $P2X_7R$-deficient mice exhibit

This article is protected by copyright. All rights reserved

Accepted Article

a baseline skeletal phenotype that includes differences in skeletal structure and mechanoresponsiveness [53]. Still, the mice clearly appeared capable of adequate osteoclastic activity during the modeling and remodeling processes of skeletal development [53]. Moreover, baseline expression of the osteocyte-associated genes that we examined were not different from wild type mice.

The current studies use an acute bone fatigue model in mice to induce osteocyte apoptosis and assess effects on pannexin-1/ P2X7 receptor-activated RANKL synthesis needed for activation and targeting of bone remodeling in response to microdamage. This experimental approach has proven to be extremely powerful in elucidating the role of osteocytes in the targeting and repair of microcracks in bone in using rat models [1,2,5,6,47], and the current data indicate that mouse bone fatigue models can be used to similar good effect. Moreover, that Panx1/P2X7 receptor-activated RANKL synthesis is required for targeted remodeling and maintenance of bone tissue material properties under physiological conditions raises the intriguing question of whether these knockout models might develop bone fragility from the absence of targeted bone remodeling. Further studies of the aging skeleton in these mice should prove intriguing. Lastly, these studies highlight some limitations of the mouse model. Kennedy et al. in our laboratory recently established using the rat ulnar fatigue model that viable bystander osteocytes near to the apoptotic ones produce RANKL.[1] This RANKL expression was triggered in the approximately 50 percent of non-dying osteocytes right near the apopototic ones and was further increased in osteocytes up to about 150 μm from microdamage sites. In the current study, we found that the apoptotic and RANKL expressing osteocytes were adjacent but discrete cells, i.e. non-apoptotic osteocytes near dying ones produce RANKL as in the rat ulna. However the spread of RANKL expression among osteocytes at some distance from the core of dying cells seen in the rat ulnae fatigue could not be assessed in the mouse ulnar cortex; the mouse ulnar cortex is too narrow to allow such extended spatial relationship to be evaluated.

Because the genetic defects in Panx1KO and $P2X_7$RKO mice are global and both genes are widely expressed [31,32,54,71], alterations in cells other than osteocytes could have contributed to the impaired RANKL expression and bone remodeling that we observed following microdamage. In particular, defects in cells of the osteoclast lineage could have contributed to the failure to form

This article is protected by copyright. All rights reserved

Accepted Article

osteoclasts and initiate resorption – one of the two endpoints we studied. Recent studies report that both Panx1 and $P2X_7R$ are required for osteoclast formation *in vitro*, consistent with this possibility [51]. However, the first endpoint we examined – RANKL upregulation – occurs extremely early in the pathway to the initiation of osteoclastogenesis. That this step was completely blocked by deficiencies in either Panx1 or $P2X_7R$ argues that this is probably the principal restriction point in the damage-induced bone remodeling pathway.

In summary, this study demonstrates a requirement for both Panx1 and $P2X_7R$ in the initiation of bone remodeling induced by skeletal microdamage. This requirement further implicates ATP as a likely signal required to trigger bystander RANKL signaling in osteocytes. Such a mechanism is consistent with signaling pathways used in other tissues to carry out apoptosis-initiated remodeling of local damage. In addition, the methods used in this study to induce microdamage in mouse ulnae should be applicable to other mouse models including knockout and transgenic strains. Furthermore, the ability to replicate the effect of genetic deficiencies by pharmacologic means using BBG indicates that these approaches can also be used in other species.

Acknowledgements

This work was supported by grants AR041210 (to MBS) and AR057139 (to MBS and DCS) from the National Institute of Arthritis and Musculoskeletal and Skin Diseases and grants DK091466 and DK081435 (to MMT and SOS) from the National Institutes of Health National Institute of Diabetes and Digestive and Kidney. We thank Damien Laudier for his expertise and guidance with histology and IHC studies, Samuel Stephen and Jessica Thomas for assistance with section preparation, Dr. Regina Hanstein for guidance with the Panx1 knockout mouse strain and Dr. Eliana Scemes for suggestions given during the course of the study. Authors contributions: MBS and DCS generated the hypothesis. WYC and MBS conducted the experiments, data collection, analyses and writing, and are responsible for the integrity of the data. SM, ZSF, JCF developed mouse fatigue model; MMT and SO

This article is protected by copyright. All rights reserved

Accepted Article

provided the mouse models and intellectual input. DCS and RJM contributed intellectual input and writing.

Accepted Article

This article is protected by copyright. All rights reserved

Accepted Article

REFERENCES

1. Kennedy OD, Herman BC, Laudier DM, Majeska RJ, Sun HB, Schaffler MB. Activation of resorption in fatigue-loaded bone involves both apoptosis and active pro-osteoclastogenic signaling by distinct osteocyte populations. Bone. 2012;50(5):1115-22.
2. Kennedy OD, Laudier DM, Majeska RJ, Sun HB, Schaffler MB. Osteocyte apoptosis is required for production of osteoclastogenic signals following bone fatigue in vivo. Bone. 2014;64:132-7.
3. Emerton K, Hu, B., Woo, AA., Sinofsky, A., Hernandez, C., Majeska, RJ., Jepsen, KJ., Schaffler, MB. Osteocyte apoptosis and control of bone resorption following ovariectomy in mice. Bone. 2010;46(3):577-83.
4. Aguirre J, Plotkin, LI., Stewart, SA.,Weinstein, RS., Parfitt, AM., Manolagas, SC., Bellido, T. Osteocyte apoptosis is induced by weightlessness in mice and precedes osteoclast recruitment and bone loss. Journal of bone and mineral research. 2006;21(4):605-15.
5. Cardoso L, Herman BC, Verborgt O, Laudier D, Majeska RJ, Schaffler MB. Osteocyte apoptosis controls activation of intracortical resorption in response to bone fatigue. Journal of bone and mineral research. 2009;24(4):597-605.
6. Verborgt O, Gibson GJ, Schaffler MB. Loss of osteocyte integrity in association with microdamage and bone remodeling after fatigue in vivo. Journal of bone and mineral research. 2000;15(1):60-7.
7. Spray DC, Hanstein R, Lopez-Quintero SV, Stout RF, Jr., Suadicani SO, Thi MM. Gap junctions and Bystander Effects: Good Samaritans and executioners. Wiley interdisciplinary reviews Membrane transport and signaling. 2013;2(1):1-15.
8. Fisher M. The ischemic penumbra: identification, evolution and treatment concepts. Cerebrovascular diseases. 2004;17 Suppl 1:1-6.
9. Garcia-Dorado D, Rodriguez-Sinovas A, Ruiz-Meana M. Gap junction-mediated spread of cell injury and death during myocardial ischemia-reperfusion. Cardiovascular research. 2004;61(3):386-401.
10. Penuela S, Kelly JJ, Churko JM, Barr KJ, Berger AC, Laird DW. Panx1 regulates cellular properties of keratinocytes and dermal fibroblasts in skin development and wound healing. The Journal of investigative dermatology. 2014;134(7):2026-35.
11. Cusato K, Bosco, A., Rozental, R., Guimaraes, CA, Reese, BE, Linden, R., Spray, D. C. Gap junctions mediate bystander cell death in developing retina. The Journal of neuroscience. 2003;23(16):6413-22.
12. Yang J, Shah, R., Robling, AG., Templeton, E., Yang, H., Tracey, KJ., Bidwell, JP. HMGB1 is a bone-active cytokine. Journal of cellular physiology. 2008;214(3):730-9.
13. Kogianni G, Mann V, Noble BS. Apoptotic bodies convey activity capable of initiating osteoclastogenesis and localized bone destruction. Journal of bone and mineral research. 2008;23(6):915-27.
14. Bidwell JP, Yang J, Robling AG. Is HMGB1 an osteocyte alarmin? Journal of cellular biochemistry. 2008;103(6):1671-80.
15. Elliott MR, Chekeni, FB., Trampont, PC., Lazarowski, ER., Kadl, A., Walk, SF., Park, D., Woodson, RI., Ostankovich, M., Sharma, P., Lysiak, JJ., Harden, T.K., Leitinger, N., Ravichandran, K.S. Nucleotides released by apoptotic cells act as a find-me signal to promote phagocytic clearance. Nature. 2009;461(7261):282-6.
16. Elliott MR, Ravichandran KS. Clearance of apoptotic cells: implications in health and disease. The Journal of cell biology. 2010;189(7):1059-70.

This article is protected by copyright. All rights reserved

Accepted Article

17. Kroemer G, Galluzzi L, Brenner C. Mitochondrial membrane permeabilization in cell death. Physiological reviews. 2007;87(1):99-163.
18. Munoz LE, Peter C, Herrmann M, Wesselborg S, Lauber K. Scent of dying cells: the role of attraction signals in the clearance of apoptotic cells and its immunological consequences. Autoimmunity reviews. 2010;9(6):425-30.
19. Peter C, Wesselborg S, Lauber K. Apoptosis: opening PANdora's BoX. Current biology : CB. 2010;20(21):R940-2.
20. Elliott M, Chekeni, FB, Trampont, PC, Lazarowski, ER, Kadl, A, Walk, SF, Park, D, Woodson, RI, Ostankovich, M, Sharma, P, Lysiak, JJ, Harden, TK, Leitinger, N, Ravichandran, KS. Nucleotides released by apoptotic cells act as a find-me signal to promote phagocytic clearance. Nature. 2009;461(7261):282-6.
21. Ravichandran KS. Beginnings of a good apoptotic meal: the find-me and eat-me signaling pathways. Immunity. 2011;35(4):445-55.
22. Ravichandran KS. Find-me and eat-me signals in apoptotic cell clearance: progress and conundrums. The Journal of experimental medicine. 2010;207(9):1807-17.
23. Luckprom P, Wongkhantee S, Yongchaitrakul T, Pavasant P. Adenosine triphosphate stimulates RANKL expression through P2Y1 receptor-cyclo-oxygenase-dependent pathway in human periodontal ligament cells. Journal of periodontal research. 2010;45(3):404-11.
24. Buckley KA, Hipskind RA, Gartland A, Bowler WB, Gallagher JA. Adenosine triphosphate stimulates human osteoclast activity via upregulation of osteoblast-expressed receptor activator of nuclear factor-kappa B ligand. Bone. 2002;31(5):582-90.
25. Korcok J, Raimundo LN, Du X, Sims SM, Dixon SJ. P2Y6 nucleotide receptors activate NF-kappaB and increase survival of osteoclasts. The Journal of biological chemistry. 2005;280(17):16909-15.
26. Koizumi K, Saitoh, Y., Minami, T., Takeno, N., Tsuneyama, K., Miyahara, T., Nakayama, T., Sakurai, H., Takano, Y., Nishimura, M., Imai, T., Yoshie, O., Saiki, I. Role of CX3CL1/fractalkine in osteoclast differentiation and bone resorption. J Immunol. 2009;183(12):7825-31.
27. Saitoh Y, Koizumi K, Sakurai H, Minami T, Saiki I. RANKL-induced down-regulation of CX3CR1 via PI3K/Akt signaling pathway suppresses Fractalkine/CX3CL1-induced cellular responses in RAW264.7 cells. Biochemical and biophysical research communications. 2007;364(3):417-22.
28. Hoshino A, Ueha, S., Hanada, S., Imai, T., Ito, M., Yamamoto, K., Matsushima, K., Yamaguchi, A., Iimura, T. Roles of chemokine receptor CX3CR1 in maintaining murine bone homeostasis through the regulation of both osteoblasts and osteoclasts. Journal of cell science. 2013;126(Pt 4):1032-45.
29. Verma SK, Leikina E, Melikov K, Chernomordik LV. Late stages of the synchronized macrophage fusion in osteoclast formation depend on dynamin. The Biochemical journal. 2014;464(3):293-300.
30. Scemes E, Spray DC, Meda P. Connexins, pannexins, innexins: novel roles of "hemi-channels". Pflugers Archiv : European journal of physiology. 2009;457(6):1207-26.
31. Baranova A, Ivanov, D., Petrash, N., Pestova, A., Skoblov, M., Kelmanson, I., Shagin, D., Nazarenko, S., Geraymovych, E., Litvin, O., Tiunova, A., Born, T. L., Usman, N., Staroverov, D., Lukyanov, S., Panchin, Y. The mammalian pannexin family is homologous to the invertebrate innexin gap junction proteins. Genomics. 2004;83(4):706-16.
32. Barbe MT, Monyer H, Bruzzone R. Cell-cell communication beyond connexins: the pannexin channels. Physiology. 2006;21:103-14.
33. Panchin YV. Evolution of gap junction proteins--the pannexin alternative. The Journal of experimental biology. 2005;208(Pt 8):1415-9.

This article is protected by copyright. All rights reserved

34. Penuela S, Bhalla, R., Gong, XQ., Cowan, KN., Celetti, SJ., Cowan, BJ., Bai, D., Shao, Q., Laird, DW. Pannexin 1 and pannexin 3 are glycoproteins that exhibit many distinct characteristics from the connexin family of gap junction proteins. Journal of cell science. 2007;120(Pt 21):3772-83.
35. Scemes E, Suadicani SO, Dahl G, Spray DC. Connexin and pannexin mediated cell-cell communication. Neuron glia biology. 2007;3(3):199-208.
36. Genetos DC, Kephart CJ, Zhang Y, Yellowley CE, Donahue HJ. Oscillating fluid flow activation of gap junction hemichannels induces ATP release from MLO-Y4 osteocytes. Journal of cellular physiology. 2007;212(1):207-14.
37. Maung S WX, Basta-Pljakic J, Schaffler M, Spray D, Suadicani S, and Thi M. Elevation of glucose to levels associated with type I diabetes impairs bone cell mechanosignaling. FASEB journal : official publication of the Federation of American Societies for Experimental Biology. 2014;28(1180).
38. Sandilos J, Chiu, YH., Chekeni, FB., Armstrong, AJ., Walk, SF., Ravichandran, KS., Bayliss, DA. Pannexin 1, an ATP release channel, is activated by caspase cleavage of its pore-associated C-terminal autoinhibitory region. The Journal of biological chemistry. 2012;287(14):11303-11.
39. Bentolila V, Boyce TM, Fyhrie DP, Drumb R, Skerry TM, Schaffler MB. Intracortical remodeling in adult rat long bones after fatigue loading. Bone. 1998;23(3):275-81.
40. Locovei S, Bao L, Dahl G. Pannexin 1 in erythrocytes: function without a gap. Proceedings of the National Academy of Sciences of the United States of America. 2006;103(20):7655-9.
41. Iglesias R, Locovei, S., Roque, A., Alberto, AP, Dahl, G., Spray, DC., Scemes, E. P2X7 receptor-Pannexin1 complex: pharmacology and signaling. American journal of physiology Cell physiology. 2008;295(3):C752-60.
42. Suadicani SO, Iglesias R, Wang J, Dahl G, Spray DC, Scemes E. ATP signaling is deficient in cultured Pannexin1-null mouse astrocytes. Glia. 2012;60(7):1106-16.
43. Negoro H, Urban-Maldonado M, Liou LS, Spray DC, Thi MM, Suadicani SO. Pannexin 1 channels play essential roles in urothelial mechanotransduction and intercellular signaling. PloS one. 2014;9(8):e106269.
44. Carter DR, Caler WE, Spengler DM, Frankel VH. Fatigue behavior of adult cortical bone: the influence of mean strain and strain range. Acta orthopaedica Scandinavica. 1981;52(5):481-90.
45. Carter DR, Caler WE. Cycle-dependent and time-dependent bone fracture with repeated loading. Journal of biomechanical engineering. 1983;105(2):166-70.
46. Frost HM. Presence of microscopic cracks in vivo in bone. Henry Ford Hosp Med Bull. 1960;8:25-35.
47. Verborgt O, Tatton NA, Majeska RJ, Schaffler MB. Spatial distribution of Bax and Bcl-2 in osteocytes after bone fatigue: complementary roles in bone remodeling regulation? Journal of bone and mineral research. 2002;17(5):907-14.
48. Hanstein R, Negoro, H., Patel, NK., Charollais, A., Meda, P., Spray, DC., Suadicani, SO., Scemes, E. Promises and pitfalls of a Pannexin1 transgenic mouse line. Frontiers in pharmacology. 2013;4:61.
49. Testa G, Schaft, J., van der Hoeven, F., Glaser, S., Anastassiadis, K., Zhang, Y., Hermann, T., Stremmel, W., Stewart, A.F. A reliable lacZ expression reporter cassette for multipurpose, knockout-first alleles. Genesis. 2004;38(3):151-8.
50. Qu Y, Misaghi, S., Newton, K., Gilmour, LL, Louie, S., Cupp, JE., Dubyak, GR., Hackos, D., Dixit, VM. Pannexin-1 is required for ATP release during apoptosis but not for inflammasome activation. J Immunol. 2011;186(11):6553-61.
51. Lemaire I, Falzoni S, Zhang B, Pellegatti P, Di Virgilio F. The P2X7 receptor and Pannexin-1 are both required for the promotion of multinucleated macrophages by the inflammatory cytokine GM-CSF. J Immunol. 2011;187(7):3878-87.

This article is protected by copyright. All rights reserved

Accepted Article

52. Dahl G, Keane RW. Pannexin: from discovery to bedside in 11+/-4 years? Brain research. 2012;1487:150-9.
53. Li J, Liu D, Ke HZ, Duncan RL, Turner CH. The P2X7 nucleotide receptor mediates skeletal mechanotransduction. The Journal of biological chemistry. 2005;280(52):42952-9.
54. Thi MM, Islam S, Suadicani SO, Spray DC. Connexin43 and pannexin1 channels in osteoblasts: who is the "hemichannel"? The Journal of membrane biology. 2012;245(7):401-9.
55. Wu D, Schaffler MB, Weinbaum S, Spray DC. Matrix-dependent adhesion mediates network responses to physiological stimulation of the osteocyte cell process. Proceedings of the National Academy of Sciences of the United States of America. 2013;110(29):12096-101.
56. Ma M, Ren Q, Zhang JC, Hashimoto K. Effects of Brilliant Blue G on Serum Tumor Necrosis Factor-alpha Levels and Depression-like Behavior in Mice after Lipopolysaccharide Administration. Clinical psychopharmacology and neuroscience : the official scientific journal of the Korean College of Neuropsychopharmacology. 2014;12(1):31-6.
57. Peng W, Cotrina, ML., Han, X., Yu, H., Bekar, L., Blum, L., Takano, T., Tian, GF., Goldman, SA., Nedergaard, M. Systemic administration of an antagonist of the ATP-sensitive receptor P2X7 improves recovery after spinal cord injury. Proceedings of the National Academy of Sciences of the United States of America. 2009;106(30):12489-93.
58. Wang Y, Cui, Y., Cui, JZ., Sun, LQ., Cui, CM., Zhang, HA., Zhu, HX., Li, R., Tian, YX., Gao, JL. Neuroprotective effects of brilliant blue G on the brain following traumatic brain injury in rats. Molecular medicine reports. 2015;12(2):2149-54.
59. Jilka RL, Noble B, Weinstein RS. Osteocyte apoptosis. Bone. 2013;54(2):264-71.
60. Li W, You L, Schaffler MB, Wang L. The dependency of solute diffusion on molecular weight and shape in intact bone. Bone. 2009;45(5):1017-23.
61. Silva MT. Secondary necrosis: the natural outcome of the complete apoptotic program. FEBS letters. 2010;584(22):4491-9.
62. Zhou Z, Han, J. Y., Xi, C. X., Xie, J. X., Feng, X., Wang, C. Y., Mei, L., Xiong, W. C. HMGB1 regulates RANKL-induced osteoclastogenesis in a manner dependent on RAGE. Journal of bone and mineral research. 2008;23(7):1084-96.
63. Silva MT, do Vale A, dos Santos NM. Secondary necrosis in multicellular animals: an outcome of apoptosis with pathogenic implications. Apoptosis : an international journal on programmed cell death. 2008;13(4):463-82.
64. Chekeni FB, Elliott, MR., Sandilos, JK., Walk, SF, Kinchen, JM., Lazarowski, ER., Armstrong, AJ., Penuela, S., Laird, DW., Salvesen, GS., Isakson, BE., Bayliss, DA., Ravichandran, KS. Pannexin 1 channels mediate 'find-me' signal release and membrane permeability during apoptosis. Nature. 2010;467(7317):863-7.
65. Poon IK, Lucas CD, Rossi AG, Ravichandran KS. Apoptotic cell clearance: basic biology and therapeutic potential. Nature reviews Immunology. 2014;14(3):166-80.
66. Kwak H, Lee, SW., Li, YJ., Kim, YA., Han, SY., Jhon, GJ., Kim, HH., Lee, ZH. Inhibition of osteoclast differentiation and bone resorption by a novel lysophosphatidylcholine derivative, SCOH. Biochemical pharmacology. 2004;67(7):1239-48.
67. Orriss I, Syberg, S., Wang, N., Robaye, B., Gartland, A., Jorgensen, N., Arnett, T., Boeynaems, JM. Bone phenotypes of P2 receptor knockout mice. Frontiers in bioscience. 2011;3:1038-46.
68. Gallagher JA. ATP P2 receptors and regulation of bone effector cells. Journal of musculoskeletal & neuronal interactions. 2004;4(2):125-7.
69. Santiago M, Veliskova, J., Patel, NK., Lutz, SE., Caille, D., Charollais, A., Meda, P., Scemes, E. Targeting pannexin1 improves seizure outcome. PloS one. 2011;6(9):e25178.
70. Bravo D, Ibarra, P., Retamal, J., Pelissier, T., Laurido, C., Hernandez, A., Constandil, L. Pannexin 1: a novel participant in neuropathic pain signaling in the rat spinal cord. Pain. 2014;155(10):2108-15.

This article is protected by copyright. All rights reserved

Accepted Article

71. Penuela S, Gehi R, Laird DW. The biochemistry and function of pannexin channels. Biochimica et biophysica acta. 2013;1828(1):15-22.

Accepted Article

This article is protected by copyright. All rights reserved

Accepted Article

FIGURE LEGENDS:

Figure 1: Summary of mouse ulnar fatigue studies. **(A)** Basic fuchsin-stained WT mouse ulnar mid diaphysis bone isolated immediately following fatigue loading; arrows show the locations of microdamage in the bone. **(B)** The enlargement region shows a fluorescence image of the microcracks (arrow) caused by the fatigue loading regime used (bar = 50 μm). **(C)** Microcrack content (Cr.Dn) in fatigue loaded ulnae vs. non-loaded ulnae and NON-MDX regions within same ulnae (FATIGUE vs No FATIGUE control, $p<0.01$). **(D)** Schematic showing principal microdamage locations (MDX) in fatigued ulnae and non-damaged (NON-MDX) regions within the same bone section. (**E and F)**: Osteocyte apoptosis (% Casp3+ Ot) and osteocyte RANKL expression (% RANKL+ Ot) in fatigued ulnae at 3 days after loading. Both osteocyte apoptosis and RANKL expression are dramatically increased, and were highly localized to the MDX regions noted in A and B (above); osteocytes in NON-MDX areas were similar to non-loaded controls (data not shown). **(G and H)** demonstrate intracortical resorption (thin arrow), endocortical tunneling site (thick arrow) and a microcrack in fatigued ulnae at 14 days post loading; this resorption is not seen in baseline mouse ulnae (bar = 50 μm).

Figure 2: Cortical bone morphology of WT, Panx1KO and $P2X_7R$ KO mice. **(A)** Micro-CT images of diaphyseal cross-sections. **(B)** Summary of micro-CT-based architectural parameters for mid-femoral diaphyses. (Tt.Ar = Total Cross-section Area; Ct.Ar = Cortical bone Area; Ma.Ar = Marrow Area; Ct.Th = Cortical Thickness; Ct.Ar./Tt.Ar = Cortical Area / Total Area; CSMI = Cross-Sectional Moment of Inertia)

Figure 3: Osteocyte apoptosis, osteocyte RANKL expression and resorption in fatigued ulnae of WT, Panx1KO and $P2X_7RKO$ mice. **(A)** Left side photomicrographs show IHC staining for osteocyte apoptosis within MDX regions of WT, Panx1KO and $P2X_7RKO$ mice at 3 days post-fatigue (bar = 25 μm) (c-Caspase 3 staining); arrows illustrate examples of positively-stained cells (brown colored).

This article is protected by copyright. All rights reserved

Right side photomicrographs show IHC staining for osteocyte RANKL expression in MDX regions at 3 days post-fatigue; RANKL staining (arrows) is evident in WT ulnae, but effectively absent from fatigued ulnae from Panx1KO and $P2X_7$RKO mice. **(B)** Histomorphometry data for osteocyte apoptosis (%Casp3+ Ot.) and osteocyte RANKL expression (%RANKL+ Ot.) in fatigued ulnae at 3 days after loading: Osteocyte apoptosis at microdamage sites occurred similarly in Panx1KO, $P2X_7$RKO and WT ulnae, consistent with IHC images shown in (A), with apoptosis increased almost 5-fold vs. NON-MDX bone areas with same bone ($p<0.02$). In contrast, osteocyte RANKL expression was absent from fatigued Panx1KO and $P2X_7$RKO bones. **(C)** Histomorphometry data for resorption space number (Rs.N) and endocortical tunneling foci number (En.Tun.N) in WT, Panx1KO and $P2X_7$RKO ulnae at 14 days after fatigue ($p<0.02$ vs WT), showing complete absence of new resorption activity in both KO strains.

Figure 4: **(A and B)** Osteocyte apoptosis and RANKL expression in fatigued mouse ulnae treated *in vivo* with the $P2X_7$R antagonist, Brilliant Blue G (BBG) or Vehicle (VEH). BBG inhibited the normal increase in osteocyte RANKL expression in ulnar cortex following fatigue loading ($p<0.05$), but did not alter the amount of osteocyte apoptosis. **(C and D)** BBG treatment dramatically reduced the activation of resorption after fatigue at both intracortical (Rs.N, $p<0.06$ vs VEH) and endocortical (En.Tun.N, $p<0.05$ vs VEH) locations.

Accepted Article

This article is protected by copyright. All rights reserved

Accepted Article

Figure 1

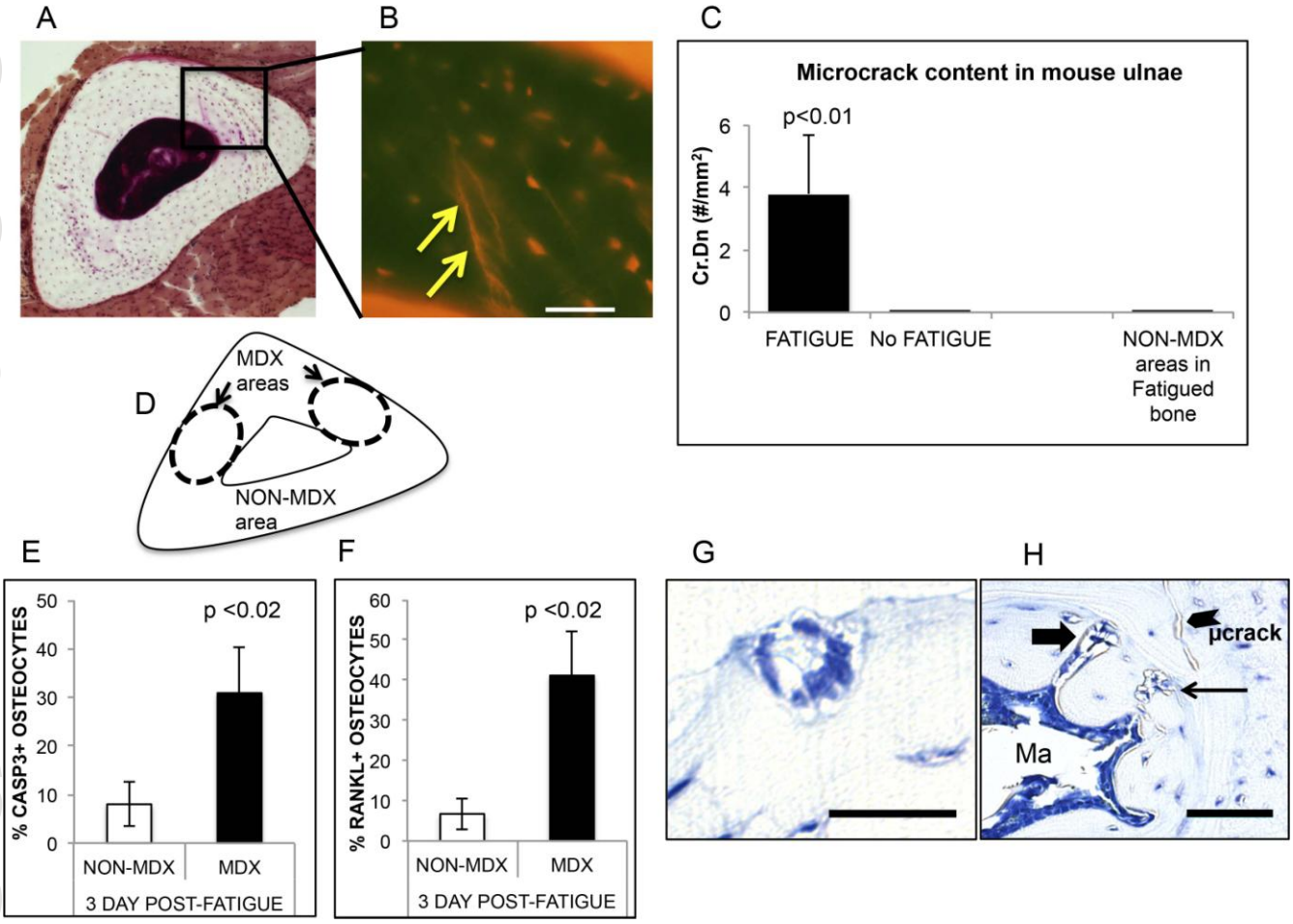

This article is protected by copyright. All rights reserved

Figure 2

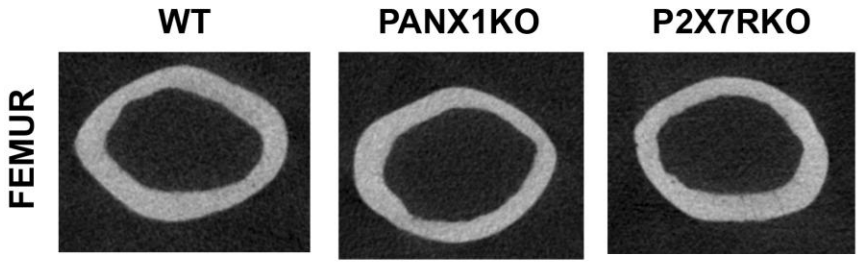

Cortical bone architecture – Femoral mid-diaphysis mean ± s.d.							
				P vs. WT			P vs. WT
PARAMETER	WT		PANX1KO			P2X7R KO	
Tt.Ar (mm^2)	1.84 ± 0.09		1.79 ± 0.04	>0.2		1.56 ± 0.04	<0.05 *
Ct. Ar (mm^2)	0.81 ± 0.06		0.81 ± 0.03	>0.5		0.85 ± 0.04	<0.07
Ma. Ar (mm^2)	1.03 ± 0.02		0.95 ± 0.02	>0.5		0.77 ± 0.11	<0.05 *
Ct. Th (mm)	0.18 ± 0.02		0.18 ± 0.01	>0.5		0.19 ± 0.002	>0.5
Ct.Ar. / Tt. Ar (%)	0.44 ± 0.05		0.45 ± 0.03	>0.5		0.50 ± 0.02	0.4
CSMI (mm4)	0.37 ± 0.01		0.35 ± 0.01	>0.4		0.30 ± 0.03	0.05 *

Accepted Article

This article is protected by copyright. All rights reserved

Accepted Article

Figure 3

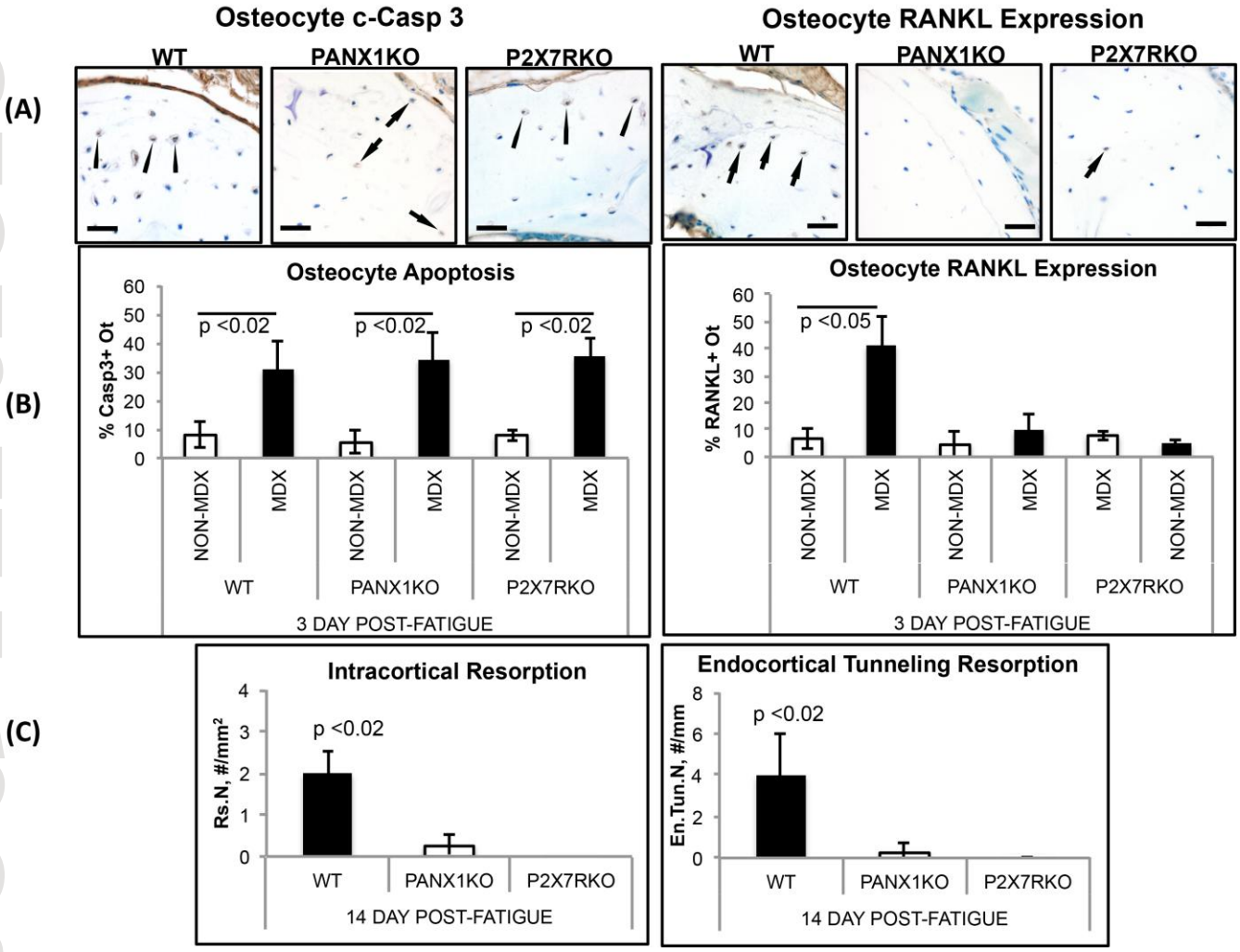

This article is protected by copyright. All rights reserved

Figure 4

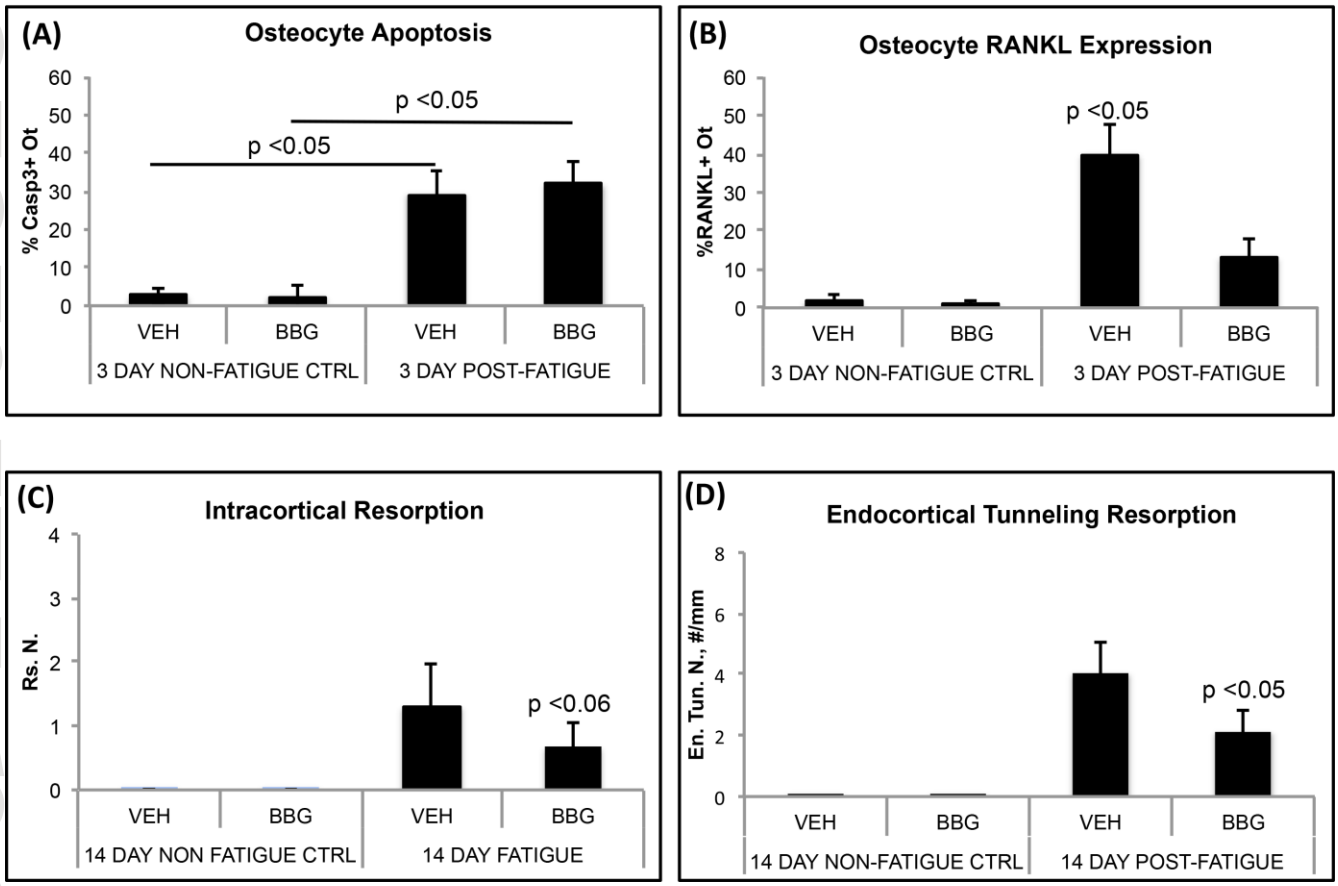

Accepted Article

This article is protected by copyright. All rights reserved